

Popular Summary for

Ocean Raman Scattering in Satellite Backscatter UV Measurements

Alexander P. Vasilkov¹, Joanna Joiner², James Gleason², Pawan K. Bhartia²

Light from the sun, reflected from the Earth's surface, passing through the atmosphere, is measured by remote sensing instruments in space. The light from the sun, the solar spectrum, is not smooth. Examined in detail the solar spectrum has a considerable amount of structure, called Fraunhofer lines, after Joseph von Fraunhofer who observed these lines in 1817. Trace species like ozone and aerosols absorb some of this light and the amount of absorbance is used to infer the amounts of these trace species in the atmosphere. The absorbance measurements compare direct light from the sun with reflected light from the Earth.

In the past it was assumed that the spectral structure from the sun, present in both the direct and reflected light cancelled out, leaving only the changes induced by the Earth's surface, absorption by gases in the atmosphere, and Rayleigh scattering by air molecules (which produces the blue color as seen with human eyes). Previous work from this group showed that this was an incorrect assumption and that small changes in the reflected Fraunhofer spectrum were caused by a different kind of scattering of the sunlight by molecules in the atmosphere, called Raman scattering. Most light undergoes Rayleigh scattering by air molecules. In this kind of scattering, the wavelength of light is not changed by the interaction with an air molecule. However, a small fraction of light is Raman scattered, which changes the wavelength of the scattered light. Due to the Fraunhofer line structure in the incoming solar light, Raman scattering causes the lines in the Earth-viewing satellite data to look filled in as compared with the incoming solar light.

This current work extends that analysis to show that there are additional changes in the changes in the reflected Fraunhofer spectrum caused by the Raman scattering of the sunlight by water molecules in the ocean. The paper describes the physical basis for the observations, the observed spectral changes, and shows how the spectral changes may be quantified to estimate the chlorophyll content in the ocean. This approach to measuring ocean chlorophyll complements existing methods, because it requires spectrally resolved measurements over a small wavelength range and is relatively insensitive to the absolute calibration of a satellite instrument.

Ocean Raman Scattering in Satellite Backscatter UV Measurements

Alexander P. Vasilkov¹, Joanna Joiner², James Gleason², Pawan K. Bhartia²

¹SSAI (please spell out)

²Laboratory for Atmospheres, Goddard Space Flight Center, Greenbelt, MD 20771

Abstract

Ocean Raman scattering significantly contributes to the filling-in of solar Fraunhofer lines measured by satellite backscatter ultraviolet (buv) instruments in the cloudless atmosphere over clear ocean waters. A model accounting for this effect in buv measurements is developed and compared with observations from the Global Ozone Monitoring Experiment (GOME). The model extends existing models for ocean Raman scattering to the UV spectral range. Ocean Raman scattering radiance is propagated through the atmosphere using a concept of the Lambert equivalent reflectivity and an accurate radiative transfer model for Rayleigh scattering. The model and observations can be used to evaluate laboratory measurements of pure water absorption in the UV. The good agreement between model and observations suggests that buv instruments may be useful for estimating chlorophyll content.

Introduction

The filling-in and depletion of solar Fraunhofer lines, known as the Ring effect [*Grainger and Ring, 1962*], is a significant component of radiances observed by backscatter ultraviolet (buv) satellite instruments. Rotational-Raman scattering (RRS) of atmospheric N₂ and O₂ is a major contributor to the Ring effect. Models for RRS have been developed and have compared well with observations from the satellite backscatter ultraviolet (SBUV) spectrometer and the Global Ozone Monitoring Experiment (GOME) [see *e.g. Joiner et al., 1995; Vountas et al., 1998*].

Properties of RRS can be exploited to retrieve cloud pressure from buv observations [*Joiner and Bhartia*, 1995; *de Beek et al.*, 2001]. Accurate modeling of the Ring effect is crucial for retrieval of cloud pressure as well as trace gas (e.g. NO₂ and SO₂) amounts from instruments such as GOME and the Ozone Monitoring Instrument (OMI) to fly on NASA's EOS Aura satellite [see e.g. *Vountas et al.*, 1998]. Derived cloud pressures from these instruments may be used to improve retrieval of total column ozone and other trace gases.

Raman scattering in the ocean has been not been included in these studies. Ocean Raman scattering has been observed and modeled in the visible spectral range [e.g. *Sugihara et al.*, 1984; *Marshall and Smith*, 1990; *Haltrin and Kattawar*, 1993; *Sathyendranath and Platt*, 1998] and causes filling in of solar Fraunhofer lines.

Figure 1 shows the ratio of the observed filling-in from SBUV continuous spectral scan measurements (taken approximately once per month from 1979-1986) to that computed using the *Joiner et al.* [1995] atmospheric RRS model over ocean scenes with low reflectivity (relatively cloud free). A similar spatial pattern with temporal variability is observed in GOME data. The filling-in over clear waters can exceed 40% of that expected from the atmosphere. There is spatial anti-correlation between the excess filling-in and chlorophyll concentrations derived from e.g. (ref). This suggests that the excess filling-in is a result of ocean Raman scattering.

In the present paper we extend existing models for ocean Raman scattering to the UV spectral range and describe a method to account for the effect in satellite buv measurements. The model is compared with data from the GOME instrument. The optical properties of water are not well known in this spectral range so that comparisons between the model and observation may be used to evaluate laboratory measurements of these properties.

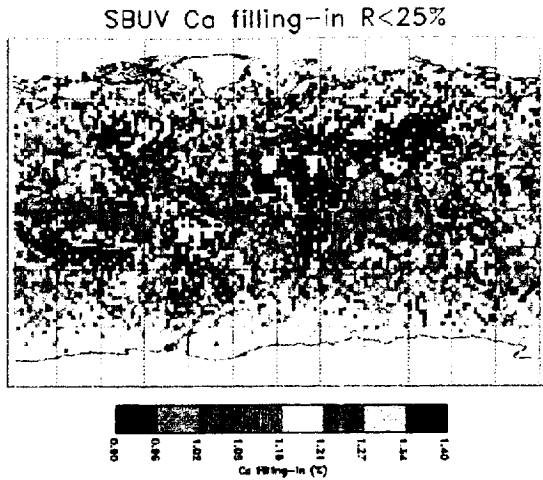


Figure 1: Excess filling-in at the Ca K line for scenes with reflectivity < 25% from SBUV continuous scan data from 1978-1986.

Ocean Raman Model

Top-of-atmosphere (TOA) radiance measured by a satellite instrument, I , can be partitioned into two components: one consisting of photons that never penetrate into water, I_a , and photons scattered at least once in water I_w , *i.e.*, $I = I_a + I_w$, where the subscripts a and w will be used to denote atmosphere and ocean, respectively. Following *Joiner et al.* [1995], we quantify the Raman scattering effect on TOA radiance by defining a filling-in factor:

$$k(\lambda) = \frac{I - I'}{I'} = \frac{I_a + I_w - (I'_a + I'_w)}{I'_a + I'_w}, \quad (1)$$

where quoted quantities denote radiances calculated with only elastic scattering. All quantities are convolved with an appropriate instrument band pass. The filling-in factor can be expressed as a sum of the filling-in factor calculated without Raman scattering in water, $k_0(\lambda)$, and the filling-in excess due to Raman scattering in water, $k_w(\lambda)$, *i.e.* $k(\lambda) = k_0(\lambda) + k_w(\lambda)$. Here, we

compute $k_0(\lambda)$ using the RRS model of *Joiner et al.* [1995]. This scheme uses the concept of Lambertian equivalent reflectivity (LER) that assumes a Lambertian reflecting surface imitating aerosol scattering, Fresnel reflection from the ocean surface, and backscatter in water. We will henceforth follow the LER concept in modeling the ocean Raman effect.

The ocean Raman scattering filling-in factor, $k_w(\lambda)$, can be expressed as a sum of two terms. The first term, $k_{w1}(\lambda)$, is positive and represents energy transferred from shorter excitation wavelengths, λ_e , to an observed wavelength λ :

$$k_{w1}(\lambda) = \frac{\int F_0(\lambda_e) \rho_w^R(\lambda, \lambda_e) d\lambda_e}{\bar{F}_0(\lambda) \rho_a(\lambda)} \approx \frac{\rho_w^R(\lambda, \lambda_e) \int F_0(\lambda_e) d\lambda_e}{\bar{F}_0(\lambda) \rho_a(\lambda)}, \quad (2)$$

where F_0 is the solar flux, \bar{F}_0 is the solar flux convolved with the instrument bandpass, and ρ is the TOA reflectance. The integration in (2) is performed over excitation wavelengths of the ocean Raman scattering band [*Haltrin and Kattawar, 1993*]. The second term, $k_{w2}(\lambda)$, is negative and is due to Raman scattering that transfers energy from the observed wavelength to longer wavelengths: $k_{w2}(\lambda) = \rho_w^R(\lambda', \lambda) / \rho_a(\lambda)$. The TOA reflectance, $\rho_a(\lambda)$, is calculated using the LER. The central wavelength of the Raman scattering band is determined by a frequency shift of $\Delta\nu=3340 \text{ cm}^{-1}$.

Assuming clear skies, the Raman TOA reflectance can be expressed in the form:

$$\rho_w^R(\lambda, \lambda_e) = \frac{T(\lambda_e, \theta_0) T(\lambda, \theta) R_{rs}(\lambda, \lambda_e)}{1 - S_b(\lambda_e) A}, \quad (3)$$

where T is the atmospheric transmittance, θ_0 is the solar zenith angle, θ is the viewing zenith angle, R_{rs} is the remote-sensing reflectance just above the ocean surface (Fresnel reflection not included), S_b is the fraction of solar flux backscattered by the atmosphere toward the ocean surface, and A is the LER. The term $1 - S_b(\lambda_e) A$ accounts for an increase of surface irradiance at

the excitation wavelength due to multiple reflections between the ocean and the atmosphere. The remote sensing reflectance can be expressed through the irradiance reflectance, R , just beneath the ocean surface. We assume isotropic angular distribution of the upwelling Raman-scattered radiance.

To calculate the Raman reflectance just beneath the ocean surface, we use the major term of the Raman reflectance formula derived by *Sathyendranath and Platt* [1998]. After some transformation this formula becomes

$$R(\lambda, \lambda_e) = \frac{b_b^R(\lambda_e)}{a(\lambda_e) + b_b(\lambda_e) + \frac{\mu_d(\lambda_e)}{\mu_u^R(\lambda)} [a(\lambda) + b_b(\lambda)]}, \quad (4)$$

where b_b^R is the Raman-backscattering coefficient, a is the absorption coefficient, b_b is the backscattering coefficient, μ_d is the mean cosine for the downwelling irradiance, μ_u^R is the mean cosine for the upwelling Raman-scattered irradiance. Because of the symmetric form of the Raman phase function, $\mu_u^R \approx 0.5$. The quantity μ_d varies between 1 and 0.5 depending on the angular structure of light incident on the ocean surface. We adopt a mean value of 0.75. To calculate the Raman reflectance of the ocean we need to specify the inherent optical properties (IOP) of seawater: b_b^R , a , and b_b .

The Raman-backscattering coefficient is half of the total Raman scattering coefficient, i.e., $b_b^R = 0.5b^R$, owing to the symmetric form of the Raman phase function. The Raman scattering coefficient has been found experimentally to vary with the emission wavelength as λ^{-5} [*Sugihara et al.*, 1984]. For excitation in the UV, the spectral dependence of the Raman scattering coefficient is $b^R(\lambda_e) \approx b_0^R(\lambda_e / \lambda_0)^{-5}$, where $b_0^R = 2.6e-4 \text{ m}^{-1}$, $\lambda_0 = 488 \text{ nm}$ [*Marshall and Smith*,

1990]. The total IOP are the sums of the IOP of pure seawater and scattering and absorbing water constituents.

At present, there is no consensus on the pure water absorption coefficient in the UV. *Pope and Fry* [1997] and *Sogandares and Fry* [1997] found that the pure water absorption coefficient is significantly lower (by a factor of two) than that given by *Smith and Baker* [1981]). Pure water absorbance substantially determines the magnitude of Raman reflectance. A comparison of the available measurements of pure water absorption in the UV is shown in Figure 2. Here, we use the interpolated data unless specified otherwise. The pure seawater backscattering coefficient is taken from *Smith and Baker* [1981].

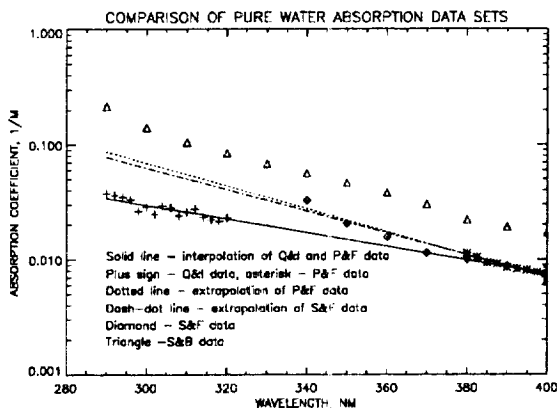


Figure 2. Available pure water absorption measurements- Q&I: *Quickenden and Irvin* [1980]; P&F: *Pope and Fry* [1997]; S&F: *Sogandares and Fry* [1997]; S&B: *Smith and Baker* [1981].

A model of IOPs in the UV is similar to one proposed by *Vasilkov et al.* [2001]. The model was updated by specifying the chlorophyll-specific absorption coefficient as a function of chlorophyll concentration. The particulate matter absorption is expressed through chlorophyll concentration, C , and the chlorophyll-specific absorption coefficient: $a_p(\lambda) = Ca_p^*(C, \lambda)$.

Parameterization of the chlorophyll-specific absorption coefficient in the UV is similar to the one

developed in the visible by *Bricaud et al.* [1995]: $a_p^*(C, \lambda) = A(\lambda)C^{-B(\lambda)}$. The coefficients $A(\lambda)$ and $B(\lambda)$ were determined from CalCOFI data sets [G. Mitchell and M. Kahru, private communication, 2001].

The IOP model contains three input quantities: the dissolved organic matter absorption coefficient at a reference wavelength, a_0 , the particulate matter backscattering coefficient at a reference wavelength, b_0 , and chlorophyll concentration, C . Chlorophyll is a standard product of ocean color sensors such as SeaWiFS and MODIS. To determine other quantities, the Case 1 water model [Morel, 1988] is assumed. According to the model, the DOM absorption at 440 nm is 20% of the total absorption of pure seawater and particulate matter pigments. This assumption determines the important parameter a_0 . The backscattering coefficient, which is normally much less than the absorption coefficient in the UV, is expressed through the total scattering coefficient. A value of the particulate total scattering coefficient at 550 nm was approximated as $b(550) = 0.3C^{0.62}$ [Morel, 1988]. Thus, all the input parameters are expressed as a function of a single input quantity – chlorophyll concentration.

Ocean Raman model calculations

In this section we present some results of calculations of k_w as a function of several parameters. All the calculations were performed using a triangular band pass with a full-width-half-maximum of 0.45 nm which is the approximate resolution of OMI. Spectral dependence of the filling in due to both atmospheric, $k_o(\lambda)$, and oceanic, $k_w(\lambda)$, Raman scattering is shown in Figure 3. For shorter wavelengths, the ocean filling-in is negative representing a net depletion of energy $k_{w2} > k_{w1}$. The opposite is true at longer wavelengths. The spectral signature is similar for $k_o(\lambda)$ and $k_w(\lambda)$. However, the magnitude of k_w decreases with λ owing to decreasing amounts of radiance reaching the surface at excitation wavelengths in the Huggins ozone band.

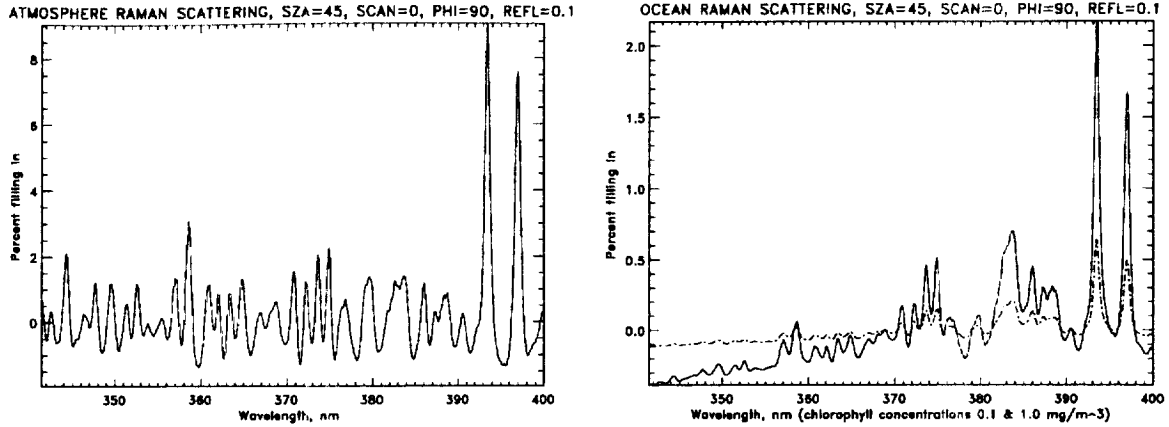


Figure 3: Right: atmospheric Raman filling-in; Left: oceanic Raman filling-in.

Figure 4 shows that k_w decreases with increasing solar zenith angle (θ_o). This dependence is different from that of atmospheric RRS that increases with increasing θ_o [Joiner *et al.*, 1995]. The decreasing the oceanic filling-in is explained by reduction of the atmosphere transmittance at excitation wavelengths with increasing θ_o .

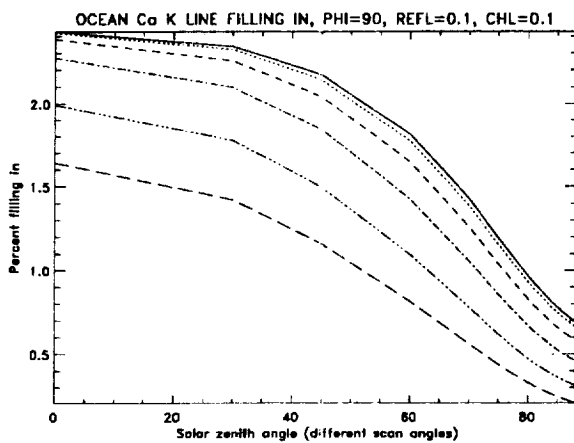


Figure 4: $k_w(\theta_o)$ for $\theta = 0, 15, 30, 45, 60,$ and 70^0 (corresponding curves from top to bottom).

Figure 5 shows that k_w diminishes rapidly with increasing chlorophyll. This illustrates that there is potential to estimate chlorophyll concentration, especially low amounts, from an instrument such as OMI.

Figure 6 shows that k_w significantly depends on the specification of pure water absorbance. In the next section, we use GOME observations to independently evaluate these laboratory measurements of pure water absorption.

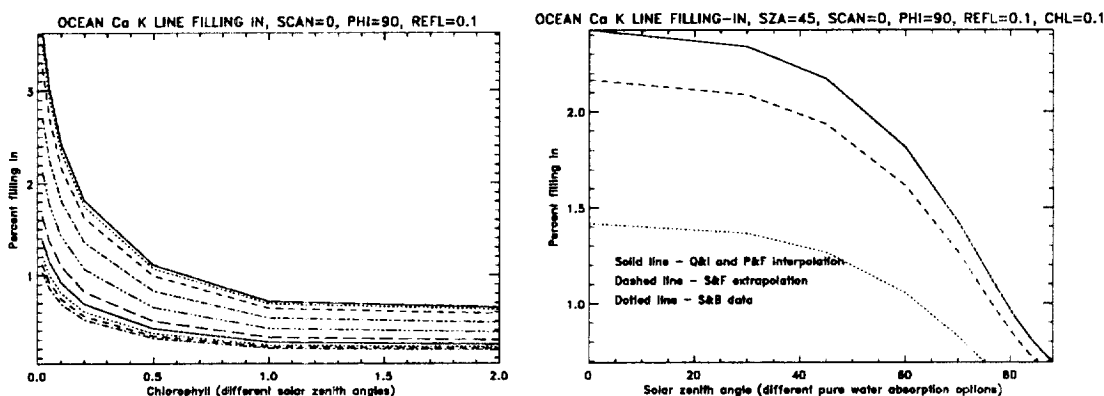


Figure 5 (left): Chlorophyll dependence of k_w for $\theta_o = 0, 30, 45, 60, 70, 77, 81, 84, 86,$ and 88^0 (corresponding curves from top to bottom).

Figure 6 (right): $k_w(\theta_o)$ for different estimates of pure water absorbance. Notations as in Figure 3.

Comparison with GOME observations

Figure 7 shows model results using climatological chlorophyll concentrations from ? compared with spectra from the GOME instrument for clear and turbid waters. The low LER reflectivities (12.6% and 6.8%, respectively) indicate relatively cloud-free pixels. In turbid waters off the coast of Mexico, model calculations with and without the ocean Raman contribution differ little. However, in the clear waters of the southern Pacific, observations show a significant difference from model calculations with only atmospheric RRS. Model calculations

with zero(climatological) chlorophyll content slightly overestimate(underestimate) the filling-in. The difference between model and observations may be due to a combination of errors in water IOPs and/or the fact that the true chlorophyll content may differ from the climatological value used here. These calculations were performed using the interpolated water absorbance from *Pope and Fry* [1997]. As Figure 6 indicates, the data are more inconsistent with the measurements of *Smith and Baker* [1981].

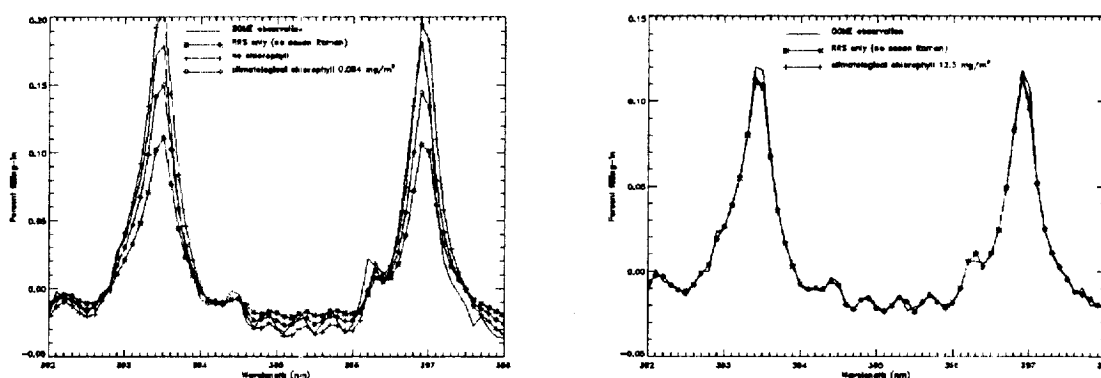


Figure 7: GOME spectra from orbit 174 on March 24, 1998 and model calculations with and without ocean Raman scattering. Left: 28°S, 121°W; Right: 21°N, 108°W.

Conclusions and Future Work

Ocean Raman scattering significantly contributes to the total filling-in of solar Fraunhofer lines over clear ocean waters. Our developed model agrees well with observations from GOME and favors the measurements of pure water absorption by *Pope and Fry* [1997]. We plan to use the model to estimate of chlorophyll concentration from satellite buv observations. This technique will utilize the spectral structure of the ocean Raman effect, which is fundamentally different from conventional ocean color algorithms and could be complementary as it has high sensitivity at low chlorophyll concentrations. An advantage of this technique is that because it uses high-

frequency spectral structure, it is less affected by errors that have a smooth wavelength dependence such calibration error.

References

de Beek R., Vountas, M., Rozanov, V. V., Richter, A., and J. P. Burrows, The Ring Effect in the cloudy atmosphere. *Geophys. Res. Lett.*, 28, 721-724, 2001.

Bricaud, A., M. Babin, A. Morel, and H. Claustre, Variability in the chlorophyll-specific absorption coefficients of natural phytoplankton: analysis and parameterization, *J. Geophys. Res.*, 100, 13321-13332, 1995.

Grainger, J. F., and J. Ring, Anomalous Fraunhofer line profiles. *Nature*, 193, 762, 1962.

Haltrin V.I. and G.W. Kattawar, Self-consistent solution to the equation of radiative transfer with elastic and inelastic scattering in ocean optics: 1. Model, *Appl. Opt.*, 32, 5356-5367, 1993.

Joiner, J., P.K. Bhartia, R.P. Cebula, E. Hilsenrath, R.D. McPeters, and H. Park, Rotational Raman scattering (Ring effect) in satellite backscatter ultraviolet measurements, *Appl. Opt.*, 34, 4513-4525, 1995.

Joiner, J. and P.K. Bhartia, The determination of cloud pressure from rotational Raman scattering in satellite backscatter ultraviolet measurements, *J. Geophys. Res.*, 100, 23019-23026, 1995.

Marshall, B.R. and R.C. Smith, Raman scattering and in-water ocean optical properties, *Appl. Opt.*, 29, 71-84, 1990.

Morel, A. Optical modeling of the upper ocean in relation to its biogeochemical matter content (Case I waters), *J. Geophys. Res.*, 93, 10749-10768, 1988.

Pope R.M. and E.S. Fry. "Absorption spectrum (380-700 nm) of pure water. II. Integrating cavity measurements," *Appl. Opt.*, Vol. 36, pp. 8710-8723, 1997.

Quickenden, T.I. and J.A. Irvin, The ultraviolet absorption spectrum of liquid water, *J. Chem. Phys.*, 72, 4416-4428, 1980.

Sathyendranath S. and T. Platt, Ocean-color model incorporating transspectral processes, *Appl. Opt.*, 37, 2216-2227, 1998.

Smith R.C., and K.C. Baker, Optical properties of the clearest natural waters, *Appl. Opt.*, 20, 177-186, 1981.

Sogandares F.M. and E.S. Fry, "Absorption spectrum (340-700 nm) of pure water. I. Photothermal measurements," *Appl. Opt.*, Vol. 36, pp. 8710-8723, 1997.

Sugihara, S., M. Kishino, and M. Okami, Contribution of Raman scattering to upward irradiance in the sea, *J. Oceanogr. Soc. Japan*, 40, 397-404, 1984.

Vasilkov, A.P., N. Krotkov, J.R. Herman, C. McClain, K. Arrigo, and W. Robinson, "Global mapping of underwater UV irradiance and DNA-weighted exposures using TOMS and SeaWiFS data products," *J. Geophys. Res.*, 106(C11), 27,205-27,219, 2001.

Vountas M., Rozanov V. V., J. P. Burrows, Ring effect: Impact of rotational Raman scattering on radiative transfer in Earth's atmosphere. *J. Quant. Spect. Rad. Trans.*, 60, 943-961, 1998.